Pers Ubiquit Comput (2013) 17:197–209
DOI 10.1007/s00779-011-0486-x

ORIGINAL ARTICLE

A performance analysis of a wireless body-area network monitoring system for professional cycling

Raluca Marin-Perianu · Mihai Marin-Perianu · Paul Havinga · Simon Taylor · Rezaul Begg · Marimuthu Palaniswami · David Rouffet

Received: 17 February 2011 / Accepted: 10 November 2011 / Published online: 27 November 2011

Abstract It is essential for any highly trained cyclist to optimize his pedalling movement in order to maximize the performance and minimize the risk of injuries. Current techniques rely on bicycle fitting and off-line laboratory measurements. These techniques do not allow the assessment of the kinematics of the cyclist during training and competition, when fatigue may alter the ability of the cyclist to apply forces to the pedals and thus induce maladaptive joint loading. We propose a radically different approach that focuses on determining the actual status of the cyclist's lower limb segments in real-time and real-life conditions. Our solution is based on body area wireless motion sensor nodes that can collaboratively process the sensory information and provide the cyclists with immediate feedback about their pedalling movement. In this paper, we present a thorough study of the accuracy of our system with respect to the gold standard motion capture system. We measure the knee and ankle angles, which influence the performance as well as the risk of overuse injuries during cycling. The results obtained from a series of experiments with nine subjects show that the motion sensors are within 2.2° to 6.4° from the reference given by the motion capture system, with a correlation coefficient above 0.9. The wireless characteristics of our system, the energy expenditure, possible improvements and usability aspects are further analysed and discussed.

R. Marin-Perianu (✉) · P. Havinga
University of Twente, Enschede, The Netherlands
e-mail: r.s.marinperianu@utwente.nl

P. Havinga
e-mail: p.j.m.havinga@utwente.nl

M. Marin-Perianu
Inertia Technology, Enschede, The Netherlands
e-mail: mihai@inertia-technology.com

S. Taylor · R. Begg · D. Rouffet
Institute of Sport Exercise and Active Living,
School of Sport and Exercise Science,
Victoria University, Melbourne, Australia
e-mail: simon.taylor@vu.edu.au

R. Begg
e-mail: rezaul.begg@vu.edu.au

D. Rouffet
e-mail: david.rouffet@vu.edu.au

M. Palaniswami
University of Melbourne, Melbourne, Australia
e-mail: palani@unimelb.edu.au

1 Introduction

As a research buzzword, pervasive computing promised to instrument the environment of the user with massive numbers of tiny embedded devices that sense, process information, communicate, take actions, render context-aware services—all with the final goal of providing support and novel functionality to the user. Gradually moving from lab prototypes to concrete products, pervasive technology is being adopted in a steadily increasing number of projects and commercial solutions, with a major visibility in the fields of entertainment, well-being and health-care. Although this is less the case in high-performance sports, the promise of "making observable the previously unseen" through all kinds of tiny wireless sensors may be appealing to athletes, sport coaches and human movement researchers, who continuously look for new solutions for enhancing performance and reducing the risk of injuries.

Cycling is one of the sports where there is a need for advanced technological means that can improve performance

and decrease the risk of overuse injuries. Numerous studies have shown that highly trained cyclists have to optimize their pedalling movement in order to maximize factors of performance such as mechanical power production and muscular efficiency, and minimize the risk of overuse injuries associated with highly repetitive movements [1, 2]. In road cycling, cyclists usually maintain their pedalling cadence around 90 rev/min, which translates into more than 20,000 revolutions in a 4-hour training ride or race and more than 80,000 revolutions in a regular week of training [2]. Pedalling movement is often optimized by fitting the bike set-up to the individual's characteristics (cleat, saddle height and tilt, stem height and length, handlebar height) [2] and from measurements undertaken in very limited time and space, so that laboratory-based motion capture systems can be used [3]. However, as fatigue occurs, the kinematics of pedalling may vary between laboratory and real-life conditions. Of primary importance is the monitoring of the knee and ankle joints, which influence the power transmitted to the pedals. Reduced ankle motion decreases knee and hip joint duty cycles, which helps diminishing the overall loss of power [1]. The knee joint angle should comply with certain limits at full extension for maximum performance [2]. While racing or training, the cyclist kinematics change in time, as a strategy to overcome fatigue [4]. Bicycle fit alone is therefore not enough to guarantee optimal performance and injury-free riding. There is a need for a portable system that can be used in real-life conditions, which can monitor continuously the kinematics of the lower limbs, process the data to detect movement alterations and provide real-time feedback that can be used to correct the pedalling technique.

We describe in the following our experiences with devising and evaluating a wireless sensing system for high-performance cyclists. Our study has the following goals:

- To design a portable wireless system that can be used for real-time monitoring of lower-limb kinematics during cycling.
- To analyse the accuracy of the system compared to the gold standard camera-based system, widely used for similar purposes in biomechanics laboratories. Due to the importance of the joint kinematics to assess the cycling technique, we focus in our study on the measurement of the knee and ankle joint angles.
- To analyse the wireless communication characteristics and their influence on the system performance.
- To analyse the energy expenditure and show the feasibility of using battery-powered wireless sensor nodes during training sessions or races.
- To extract a series of usability aspects from our interviews with cyclists and sport scientists.

The rest of the paper is organized as follows. In Sect. 2, we give a review of the related work. We present the solution overview in Sect. 3. Experiments and results are described in Sects. 4 and 5. Section 6 gives a detailed discussion of results, possible improvements and usability aspects. Finally, Sect. 7 concludes the paper.

2 Related work

Targeted to improve performance and obtain optimal physical fitness, commercially available cycling equipment is becoming more and more sophisticated. For instance, Polar cycling accessories [5] include features for heart rate monitoring, cadence, speed, distance, calorie consumption, temperature, uphill or downhill steepness and route information in mapping software.

Research directions in the field of cycling cover sensing systems and laboratory-based motion analysis. Similar to the Polar equipment, the BikeNet [6] sensing system collects and stores the current and average speed of the cyclist, the distance, the calories burned, the path incline, the heart rate and the galvanic skin response. To provide these measures, a number of sensors are installed on the bicycle, such as magnetometer, microphone, inclinometer, GPS etc. The BikeNet software allows long term performance trend analysis, local and remote presentation of collected data.

Laboratory-based motion analysis systems [7] use optical inputs from markers attached to the entity in motion and captured by cameras. Experiments have been conducted in laboratory environments to study the body segment kinematics during regular cycling [3] or to assess the changes in kinematics during fatigue [1, 4]. However, since experiments are confined in time and space, these systems are not an option for long-term, outdoors experiments.

Miniaturized sensing systems have become potential alternative solutions to the camera systems. These systems have to be small enough to facilitate outdoor usage and accurate enough to provide reliable measures. Inertial sensors, such as accelerometers and gyroscopes, combined with magnetometers and other kinetic-related sensors, can provide detailed motion information, but less accurate than camera systems. A common problem of the inertial sensor systems is that of error accumulation in time from the integration of the sensor signal, due to the electronic bias error and the deviation from the sensing axis [8].

The methods for error compensation range from elaborated filtering techniques to exploiting the human motion characteristics based on a particular application. For example, Luinge and Veltink [9] use a Kalman filter to make an estimate of the orientation error, using a combination of accelerometer and gyroscope signals. Similarly, Zhu and Zhou [10] propose a Kalman filter-based algorithm, which integrates accelerometer, gyroscope and magnetometer signals and gives a stable drift-free performance. However,

they acknowledge that the Kalman algorithm causes a time lag in a real application, which is difficult to overcome. Roetenberg et al. [11] uses a portable magnetic actuator that emits short magnetic pulses. These pulses are received by magnetic sensors and are related to the distance to the transmitter. This magnetic tracking system is used in combination with an inertial navigation system as an input to a Kalman filter to compute a minimum error estimate of the system state.

The analysis of human body biomechanics using wired inertial sensors has been studied especially in the field of healthcare. For example, kinematic and kinetic measurements are widely used for gait analysis. Morris [12] proposes a wireless system for real-time gait analysis integrated in the shoe. One of the methods for error compensation used by Morris is the assumption that the velocity of the shoe is zero during the period when the foot is on the ground. An approach for the measurement of joint angles is proposed by Dejnabadi et al. [8], which uses accelerometers and gyroscopes to estimate the acceleration at the joint centre of rotation. For minimizing the error, they obtain accurate positions of the physical sensors, and thus the model is personalized for each subject it turn. Findlow et al. [13] propose a model that predicts the lower limb kinematics based on partial data, using a generalised regression neural network. However, an accurate prediction requires extensive training of the neural network. Another method is proposed by Takeda et al. [14], where the joint angles are computed from the inclination given by the accelerometer signal. For simplification, the authors neglect the transitional acceleration, while considering only rotational motion, which can be computed using the gyroscope data.

Compared to the state-of-the-art research in the field, we propose a new approach for the real-time monitoring of the human body kinematics during cycling. The specific novel contributions are as follows:

- The system is *portable*, being composed of wireless sensor nodes. The lack of wires makes performance analysis possible outside the lab, which is an important demand from athletes and coaches.
- The system is *distributed* due to its wireless nature. This means that multiple kinematic parameters can be monitored at different positions and furthermore fused for computing more complex measures. More granular and detailed information is thus possible at a reduced cost.
- The algorithm for computing the orientation angles proposes an *innovative* way of fusing the data from the accelerometer, gyroscope and compass sensors. Most of the related work in inertial sensing focuses on elaborated filtering techniques, which are not feasible for the resource-constrained hardware of sensor nodes. The algorithm we propose exploits the cyclic nature of the motion and introduces a reset step for avoiding the accumulation of integration errors. The algorithm is *lightweight*, *feasible to run* on low-power micro-controllers and *accurate* with respect to the reference camera system.

3 Solution overview

3.1 Wireless sensing system

The sensing system (see Fig. 1) is composed of several body area wireless inertial sensor nodes based on the ProMove platform [15]. ProMove creates a bridge between inertial measurement units (IMUs) and wireless sensor networks (WSNs) by embedding in one device the following:

- 8 degrees-of-freedom inertial sensors: ±1.5 to 6 g three-axial accelerometer, ±500°/s two-axial gyroscope and 6 gauss three-axial magnetometer.
- Low-power MSP430 micro-controller, widely used in "motes"-like sensor node platforms.
- IEEE 802.15.4-compliant system-on-a-chip (SoC) for low-power wireless networking.

The micro-controller is dedicated for sampling the inertial sensors and running specific data processing algorithms. The SoC provides the developer with the necessary computational and memory resources for implementing the wireless networking protocol stack. This facilitates a two-tier approach and a beneficial separation of resources between sensor data processing and wireless networking.

3.2 Measurement of kinematic parameters

As shown in Fig. 2, we use three ProMove nodes placed along the left leg of the cyclist, on the thigh, shank and foot. For each node, we compute its orientation relative to

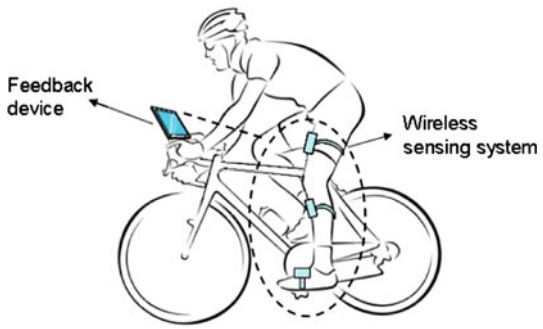

Fig. 1 Wireless inertial sensing system overview: strap-on wireless sensor nodes and wireless feedback device

Fig. 2 Subject wearing the ProMove nodes

the Earth reference frame in terms of roll, pitch and yaw (R-P-Y) angles. By combining the orientation of each node, we obtain the joint motions of the three segments of the lower limb. In our current experiments the kinematic parameters of interest are the *knee* and *ankle* joint angles, noted with K and A, respectively. As depicted in Fig. 3, both K and A can be computed from the roll angles derived from the motion of the three nodes in the sagittal plane, as follows:

$$\begin{aligned} K &= \pi - R_1 - R_2 \\ A &= R_2 + R_3 \end{aligned} \tag{1}$$

The measurement process can be therefore divided in two steps: (1) the computation of the orientation of each node and (2) the determination of the joint angles.

3.2.1 Orientation computation

At any given time, the stationary condition is detected by analyzing the variance of the acceleration magnitude over a sliding time interval. If the variance is below a given threshold, then the node is considered stationary and its orientation is computed using the accelerometer and compass readings: considering that a_x, a_y and a_z are the projections of static acceleration on x, y and z axis (i.e. the readings of the accelerometer sensor), the roll and pitch angles are computed as follows [16] (see also Fig. 4a):

$$\begin{aligned} R &= \arctan\left(\frac{a_y}{\sqrt{a_x^2 + a_z^2}}\right) \\ P &= \arctan\left(\frac{a_x}{\sqrt{a_y^2 + a_z^2}}\right) \end{aligned} \tag{2}$$

Considering that c_x, c_y and c_z represent the projections of the magnetic field on the three axes (i.e. the readings of the compass sensor), then the yaw angle Y is computed as follows [17] (for brevity we use the short trigonometric notations $c\alpha$, $s\alpha$, $t\alpha$ to denote the cos, sin, tan of angle α):

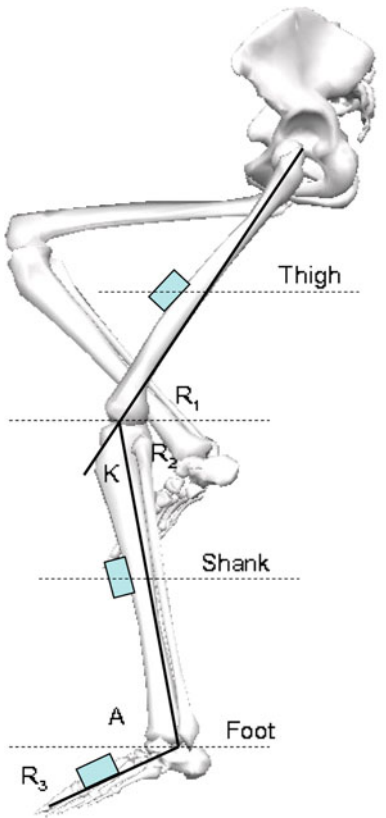

Fig. 3 Diagram of the cyclist's thigh, shank and foot and the corresponding roll angles

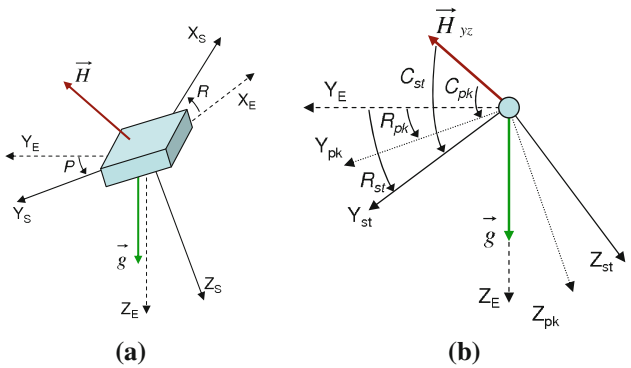

Fig. 4 **a** Diagram of the sensor rigid body (axes identified with subscript S) with respect to the Earth reference frame (axes identified with subscript E). Gravity $\overline{g}$, magnetic field $\overline{H}$ and tilt angles roll R and pitch P are also represented. **b** Determination of the new roll angle R_{pk} at pedal-up position using the projection of the magnetic field in the saggital plane and the values computed during the most recent stationary position

$$Y = \arctan\left(\frac{c_x cR + c_z sR}{c_y cP + (c_x sR - c_z cR)sP}\right) \quad (3)$$

During cycling (i.e. when the variance of the acceleration magnitude exceeds the given threshold), the R-P-Y angles are updated using the gyroscope readings g_x, g_y and g_z. Given the fact that the nodes have only a 2D gyroscope, the angular velocity g_z is assumed 0. Using the rotation matrix [18]:

$$M = \begin{pmatrix} 1 & tPsR & -tPcR \\ 0 & cR & sR \\ 0 & -sR/cP & cR/cP \end{pmatrix} \quad (4)$$

we compute the new angles R', P' and Y':

$$\begin{pmatrix} R' \\ P' \\ Y' \end{pmatrix} = \begin{pmatrix} R \\ P \\ Y \end{pmatrix} + M \begin{pmatrix} g_x \\ g_y \\ 0 \end{pmatrix} \quad (5)$$

A well-know problem of Eq. 5 is the effect of error accumulation due to the integration of the gyroscope data. During stationary periods, the orientation angles can be reset to the values computed through Eqs. 2 and 3, but while moving the errors can accumulate in time indefinitely. Our approach to this problem is to exploit the repetitive pattern of the cycling motion and to reset the orientation angles to values computed from the compass readings. The advantage of the compass sensor is that it gives an absolute attitude measure, without suffering from error accumulation. The disadvantage is represented by possible disturbances of ferrous or magnetic nearby structures, but this problem is relatively minor in our case because most modern bikes have lightweight non-metallic structures. For a more detailed discussion on these aspects, see Sect. 6.

The reset is applied when the lower limb is at the pedal-up position, which corresponds to a minimum peak in the roll angle. If we denote with *st* the values obtained during the most recent stationary period (using Eq. 2) and with *pk* the values when reaching the pedal-up position, we compute the new roll angle (see also Fig. 4b):

$$R_{pk} = R_{st} - C_{st} + C_{pk} \quad (6)$$

where $C_{st} = \arctan(\frac{c_{z,st}}{c_{y,st}})$ and $C_{pk} = \arctan(\frac{c_{z,pk}}{c_{y,pk}})$.

The pitch angle is assumed to remain unchanged, i.e. $P_{peak} = P_{static}$ and the new yaw angle Y_{peak} is derived using R_{peak} and P_{peak} in Eq. 3 (see Sect. 6 for a discussion of this assumption). Until the next pedal-up position, the integration step continues as in Eq. 5.

3.2.2 Joint angles

As described in Eq. 1, the *knee* and *ankle* joint angles can be determined using the absolute roll angles from all three nodes. This means that the nodes have to exchange the roll angle values among them, while also interacting with the feedback device. If we denote by D the feedback device and by T, S and F the node on the thigh, shank and foot, respectively, we have the following possibilities:

1. T, S and F compute the roll angles and send them periodically to D, which determines the joint angles.
2. S broadcasts periodically its roll angle, T determines the joint angle K and sends it to D, S determines the joint angle A and sends it to D.
3. T and F send periodically their roll angles to S, S determines both joint angles and send them to D.

Each of these strategies has its advantages and drawbacks, in terms of computational effort and wireless communication overhead. Depending on the hardware resources available on the feedback device, the first strategy is preferred because:

- There is less computational effort and less communication overhead for the nodes (the nodes only have to transmit their data to D, without any inter-node communication that would further complicate the medium access protocol).
- The nodes run the same algorithm, in other words there is no specialization among nodes.
- D can ensure a proper synchronization among the data received from the nodes, for example by arbitrating the medium access in a TDMA manner and imposing sequence number matching. Data synchronization is an essential point for a correct measurement procedure, as any mismatch between the absolute angle information can produce erroneous results in the joint angles.

4 Experiments

4.1 Objectives

The main objective of our experiments is to validate the performance of the measurement algorithm presented in Sect. 3.2, using the ProMove sensor nodes, with respect to the reference camera system. In addition, we would like to investigate possible optimizations of the data processing and to evaluate the quality of the wireless communication.

To achieve these objectives, we focus in the experiments on the following tasks:

- Collect all the raw data from all sensors to a central computer, at the highest possible data rate via the wireless medium.
- Process the data on the computer and optimize the algorithms for the trade-off between accuracy and

Table 1 Participants details

No.	Gender	Age	Height (cm)	Body mass (kg)	Cycling
1	M	30	172	80	Commuting
2	M	31	180	73	Recreational
3	F	24	164	54	Commuting
4	F	22	166	64	Recreational
5	M	30	172	62	Commuting
6	M	23	182	68	Competition
7	F	30	172	50	Commuting
8	M	25	181	76	Commuting
9	M	38	185	90	Commuting

computational overhead (the algorithms have to be eventually implementable on the sensor nodes).
- Evaluate the quality of the wireless communication and identify adverse factors.
- Compare the results obtained with the sensor nodes to the ones supplied by the reference system.
- Run the experiments with multiple subjects and various bikes, to verify the generality of our approach.

4.2 Sensor sampling and communication

Sampling at high rates ($\geq$100 Hz) the inertial sensors and communicating all the raw data is difficult due to the limited hardware available on sensor nodes (see recent work of Bosch et al. [19] for a detailed discussion of practical problems). The ProMove nodes alleviate the problems to a large extent, by providing the full power of the MSP430 micro-controller for handling the sensors, while the wireless communication protocols can run separately on the SoC.

During initial tests we found the IEEE 802.15.4 implementation to be inappropriate for gathering data from all three nodes at the desired rates. Therefore, in our experiments we use a specialized MAC protocol developed for ProMove nodes, FastMAC, with which we can collect data from all the inertial sensors at rates of up to 250 Hz, with synchronization among nodes in the range of microseconds. It is important to mention that FastMAC could be also used to implement the communication strategy described at the end of Sect. 3.2.2, possibly at a much lower duty cycle. However, a good synchronization among the nodes is essential in all cases, as the computation of the joint angles has to use orientation information derived from all nodes at the same time instance.

4.3 Experimental setting

Nine subjects participated in our experiments (6 male and 3 female), one being a semi-professional cyclist (see Table 1). All subjects performed the test with their own bikes positioned on roller cylinders. For non-professional cyclists, the bike was secured and a support was provided to them to ensure their total safety (see Fig. 5a). For the cyclist, both wheels revolved on the cylinder roller and he balanced his bicycle just as if he was riding normally (see Fig. 5b). Each experiment consisted of five sessions corresponding to five pedalling cadences: 40, 60, 80, 100 and 120 rpm. In each session the subject was asked to cycle for one minute at a target cadence. As a final experiment, the semi-professional cyclist performed a ride of approximately five minutes at free cadence, in order to verify the robustness of our solution to sensor drift and accumulation of errors.

We collected data from both the sensor nodes and the reference motion analysis system (Optotrak Certus, Northern Digital Inc. [7]). The Optotrak system was used as a gold standard laboratory approach. Infra-red markers placed at the anterior surface of the mid-thigh, the anterior surface of the mid-shank and the superior surface of the mid foot on the left lower limb were tracked while subjects were pedalling. A non-collinear marker cluster technical frame composed of four tracking markers was created with the unit sensors serving as a rigid structure to define an arbitrary three-dimensional orthogonal segment coordinate system [20]. Using the foot, shank and thigh tracking markers and their respective distal and proximal anatomical landmarks, Visual3D model building software [21] was used to reconstruct anatomically meaningful segment coordinate system.

Data was sampled at 200 Hz for both the sensor nodes and the camera system. Before each experiment (i.e. once for each subject), both the sensor nodes and the camera system were calibrated. For the sensor nodes, we calibrated the static acceleration using the method described in [22] and the magnetic compass using the method presented in [23]. We chose these methods for their simplicity (complete calibration of the three nodes takes about 5 min), as it is not realistic to assume that users would be willing to go through intricate calibration procedures.

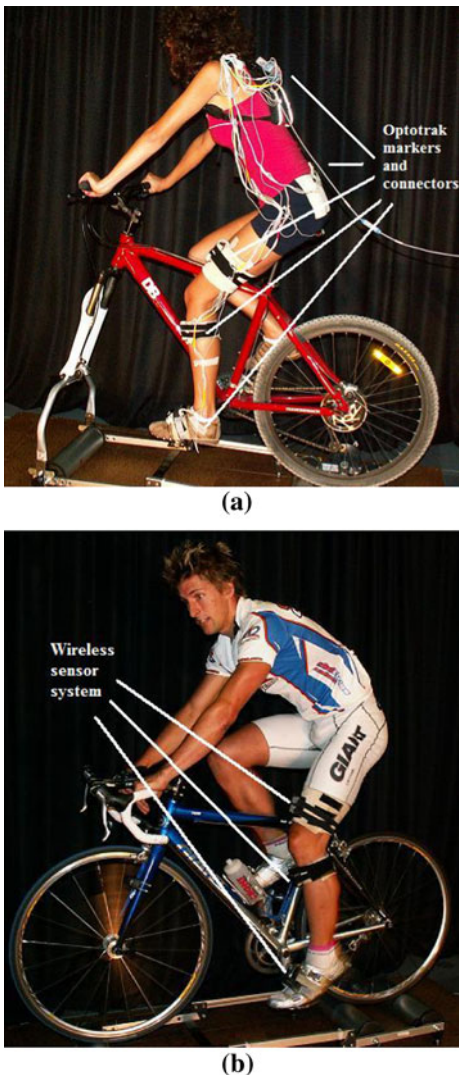

Fig. 5 Experimental setting. **a** Subject wearing the Optotrak camera markers and the ProMove nodes. **b** Subject wearing only the ProMove nodes

The raw data obtained from sensor nodes was processed on the computer using Matlab, in order to derive the joint angles defined in Sect. 3.2. The accelerometer and compass are used to establish the orientation of each node (R-P-Y angles) in static mode, at the beginning of each experimental session. During cycling, the gyroscope and compass are used to measure the variation of the roll angle and subsequently compute the joint angles. The processing algorithm is kept lightweight so that it is feasible to implement on sensor nodes. For determining the measurement accuracy of the joint angles using sensor nodes, we use as reference the values provided by the Visual3D software.

A sample video of one experiment showing data collection from the wireless sensor nodes is available at [24].

5 Results

We start this section with a snapshot of a sample experiment, which we use to illustrate the typical waveform signals and to introduce the measures of interest. Next, we present the detailed accuracy results. Finally, we provide a characterization of the wireless communication performance.

5.1 A typical experimental session

Figure 6 shows a portion of around 7 s from an experiment performed at 100 rpm. For all the plots, the horizontal axis represents the time in seconds and the vertical axes depicts the angle in degrees computed both by our algorithm using the wireless sensor nodes (continuous line) and the reference Optotrak system (dotted line).

The first three plots compare the absolute thigh, shank and foot angles, as measured by the two systems. We notice the clear repetitive pattern, with ranges of motion of approximately 40°. We also observe that the actual cadence achieved by the subject is about 94 rpm. The bottom plots show the joint knee and ankle angles, computed as explained in Eq. 1. In particular, plots 5 and 7 show the peaks of the joint angles. We notice that the results of our algorithm follow closely the Optotrak reference, with small differences in the signal amplitude, which are reflected in the differences between peaks. Even if the signal has small disturbances, for example between seconds 5 and 6 for the ankle angle, our system manages to reproduce it quite accurately. Interesting to notice is the reset procedure, which occurs for example just before second 8 in the foot angle, and which is reflected in a sudden shift of the signal in the ankle angle.

5.2 Accuracy results

We use three measures for establishing the accuracy of our system versus Optotrak, with respect to the determination of the joint knee and ankle angles:

- The root mean square error (RMSE) for the peak angles (peak values are shown in plots 5 and 7 of Fig. 6). These values are important measures for the cycling performance [2].
- The RMSE for all the joint angle values (joint angle values are shown in plots 4 and 6 of Fig. 6).
- The correlation coefficient for all the joint angle values.

Figure 7 shows the RMSE values computed for each experiment (cadence and subject). Figure 7a shows the errors at the peak values, while Fig. 7b summarizes the errors for all the values of the joint angles. The results are grouped horizontally based on the cadence. Each plot shows in the left half the knee angle RMSE values and in

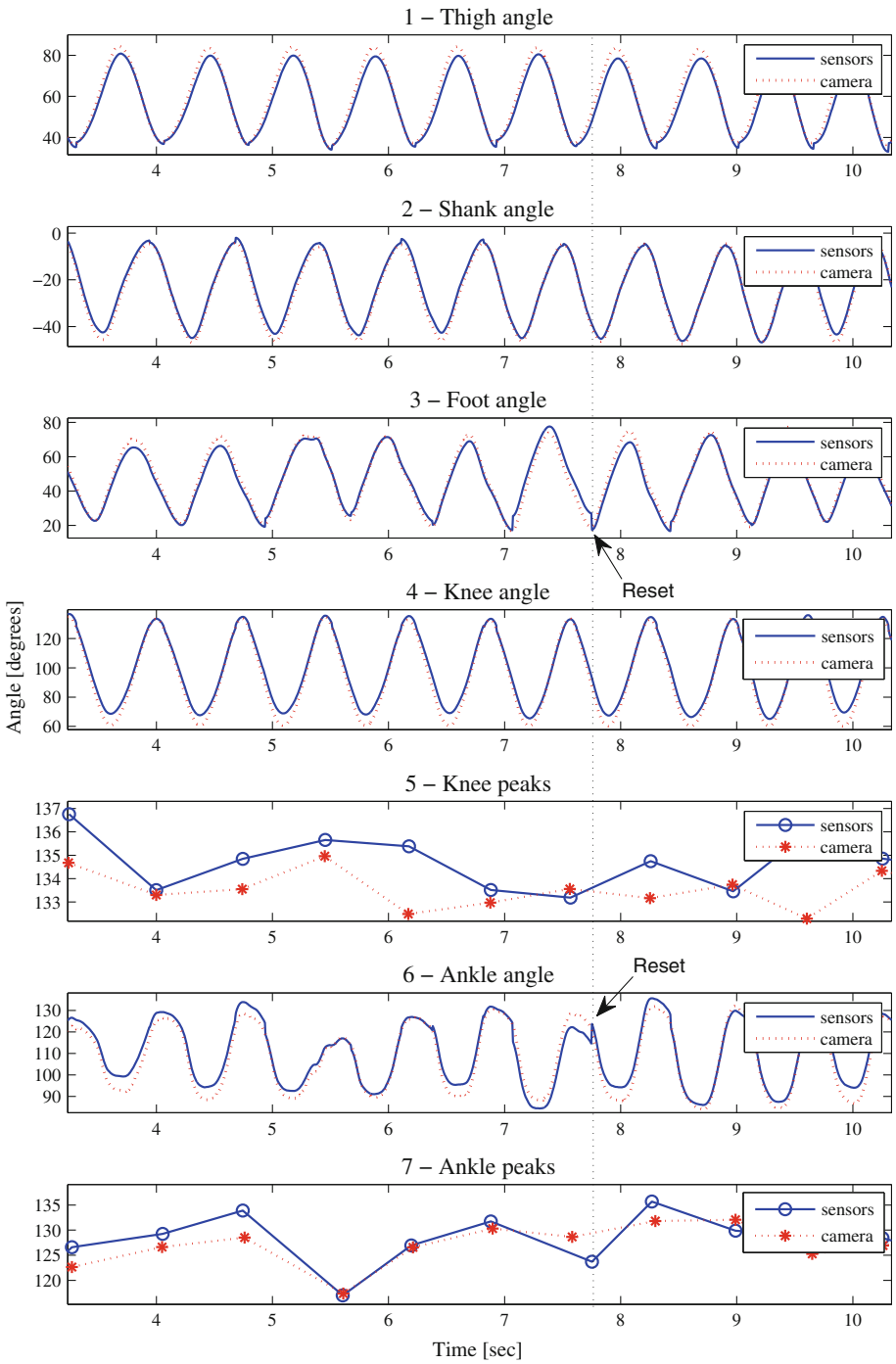

Fig. 6 Sample experiment at 100 rpm, showing the computation of the thigh-shank and shank-foot angles and peaks, from the individual thigh, shank and foot angles. The plots show the comparison between the angles computed by the reference Optotrak system and those using the wireless ProMove nodes

the right half the ankle angle RMSE values, for all the nine subjects that participated in the experiments (subject number 6 is a semi-professional cyclist).

The summary results are shown in Tables 2 and 3. The means of the RMSE values and correlation coefficient for all subjects are presented depending on the cadence. The last line in each table gives the global mean results for all subjects and cadences.

Based on these results, we conclude the following:

- Our system measures the joint angles at peak positions with RMSE 2.28° for the knee angle and 4.77° for the ankle angle. The larger error in the ankle angle is most probably due to the magnetic field influences present in the experimental lab. Our measurements using a conventional compass indicated that the magnetic field varied widely in the vertical plane, with strong

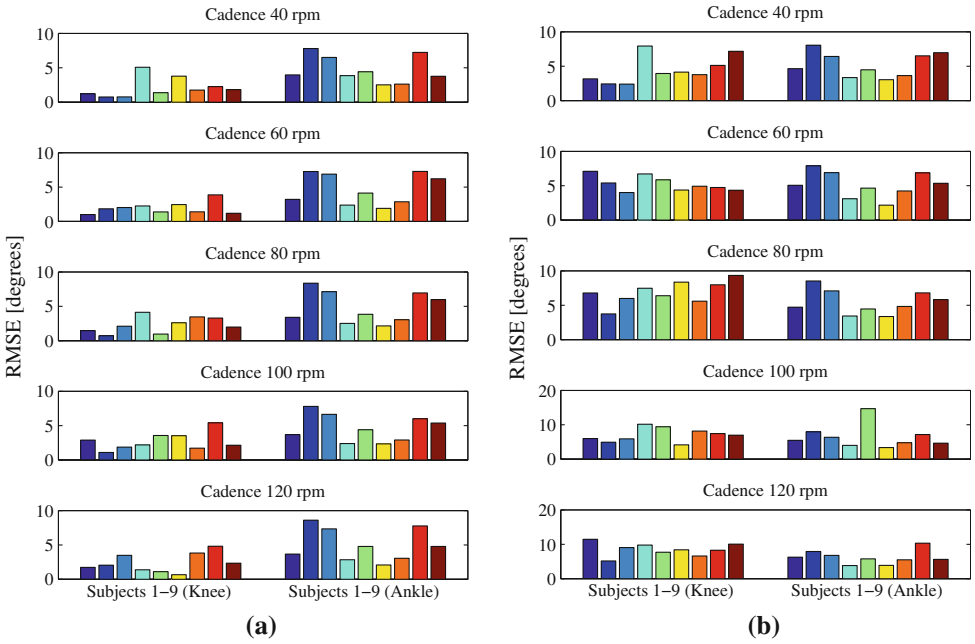

Fig. 7 RMSE values characterizing the differences between the sensors and the Optotrak system. The values are shown for the knee and ankle joint angles, for all subjects and cadences. **a** Errors at the peak values. **b** Errors for all the values of the joint angles

Table 2 Knee angle summary results

Cadence (rpm)	RMSE peaks (degrees)	RMSE all (degrees)	Corr. coef. [−1:1]
40	2.09	4.45	0.991
60	1.93	5.27	0.986
80	2.30	6.85	0.974
100	2.71	7.01	0.974
120	2.37	8.49	0.957
Mean	2.28	6.41	0.976

Table 3 Ankle angle summary results

Cadence (rpm)	RMSE peaks (degrees)	RMSE cont. (degrees)	Corr. coef. [−1:1]
40	4.75	5.23	0.904
60	4.68	5.13	0.921
80	4.82	5.45	0.919
100	4.61	6.48	0.890
120	4.99	6.20	0.911
Mean	4.77	5.70	0.909

disturbances close to the floor level (a network of electricity wires was laid down below the floor). This means that the node placed on the foot was particularly exposed to such disturbances.

- Our system measures the overall joint angles with RMSE 6.41° for the knee angle and 5.70° for the ankle angle. The larger error in the knee angle is explained by the larger range-of-motion (RoM) of this joint. As shown by plots 4 and 6 of Fig. 6, the RoM for the knee angle is approximately 70°, while the RoM for the ankle angle is less than 40°.
- The correlation coefficients for the knee angles are higher than for the ankle angles. This indicates that the knee angle signals obtained with the sensors are closer to the ones provided by Optotrak in terms of pattern similarity. While the knee angle exhibits a rather smooth sinusoidal pattern, the ankle angle is more noisy. Additionally, the reset procedure depicted in plot 6 of Fig. 6, which applies only to the results provided by the sensor system, also contributes to a lower value of the correlation coefficient for the ankle angle.

Figure 8 gives a snapshot of the results obtained in our last experiment, where the semi-professional cyclist performed a ride of approximately five minutes at free cadence. The purpose of this experiment was to verify the robustness of our solution to known issues of inertial sensors, such as drift and accumulation of errors. The plots show the peak values of the knee and ankle angles during approximately one minute at the beginning of the experiment (left) and at the end of experiment (right). The results confirm that there is no significant drift or accumulation of errors in time, due to the reset procedure applied every cycle. The RMSE values for the overall experiment remain in-line with the results obtained for the one-minute experiments, for example 2.43° for knee angle peak values and 3.38° for ankle angle peak values.

5.3 Wireless communication

Along with the sensor data, we collect information related to the received signal strength indication (RSSI) and sequence numbers of each radio packet. The latter allows

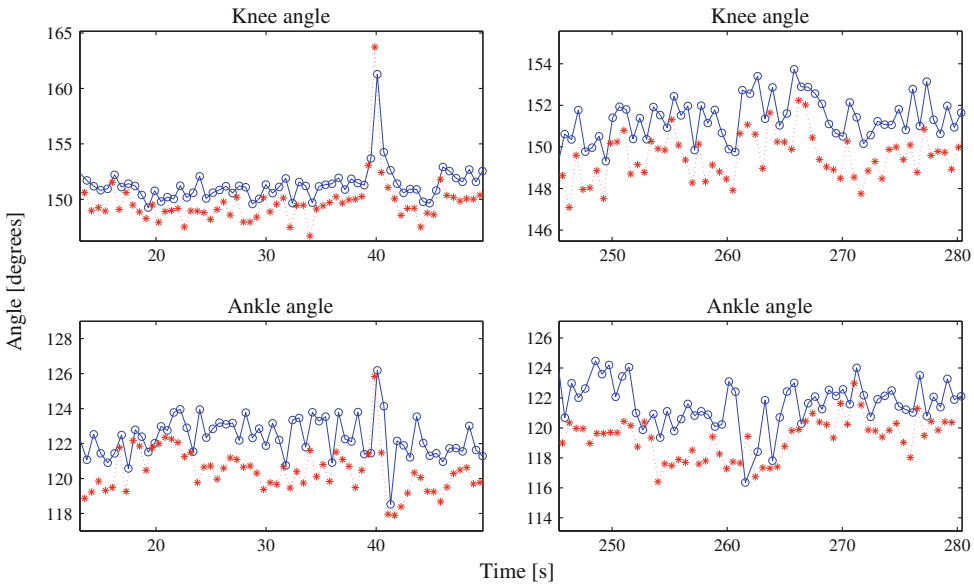

Fig. 8 Experiment of riding 5 min with free cadence. The plots compare the peak values of the knee and ankle angles between the ProMove nodes and the Optotrak system: *left plots* show the first minute of the experiment, *right plots* show the final minute of the experiment

us to identify lost packets and fill in the gaps in the data using linear interpolation.

Figure 9a gives an example of how the RSSI varies during a typical experiment. The information is collected from the node on the thigh. We observe the clear repetitive pattern following closely the pedal revolution motion. The frequency of the low peaks corresponds to approximately 57 rpm and proves to be a reliable indicator of the pedaling cadence (the metronome was set to 60 rpm in this experiment). Figure 9b summarizes the RSSI values for all

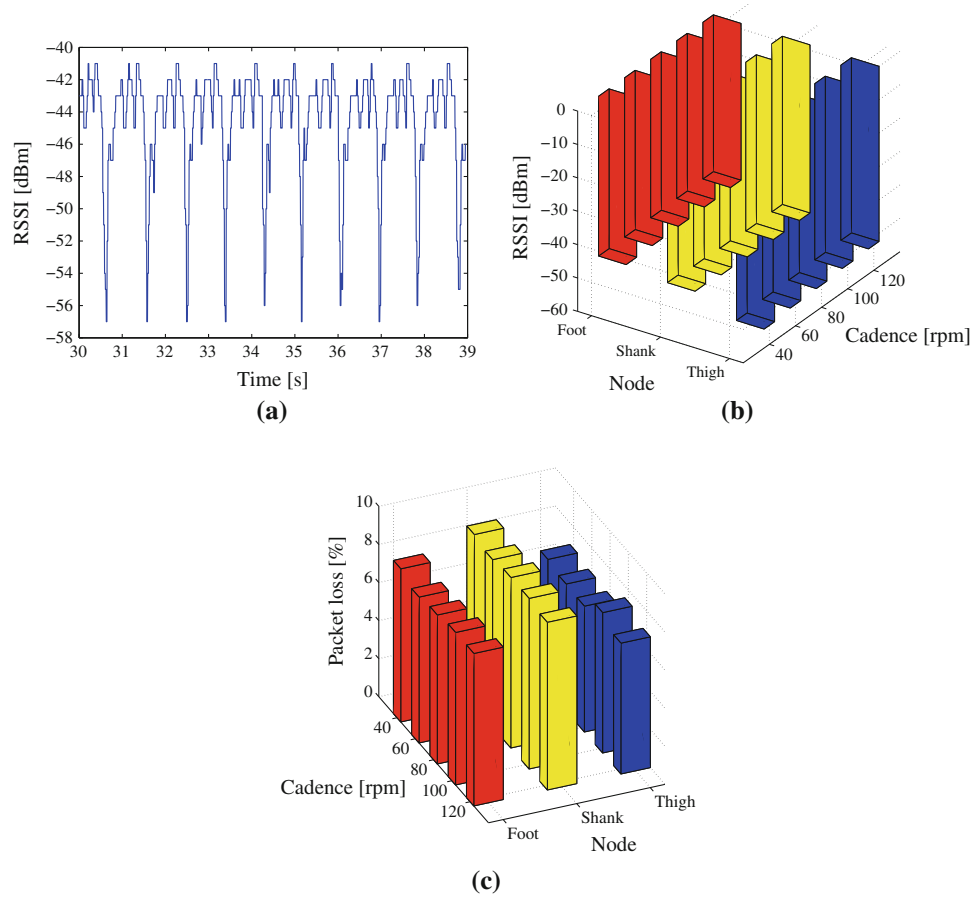

Fig. 9 **a** RSSI variation in a sample experiment at 60 rpm. **b** Overall RSSI results. **c** Overall packet loss rates

subjects, for each node and cadence. The overall mean RSSI values are −53, −50 and −48 dBm for the thigh, shank and foot node, respectively. The nodes on the thigh and foot exhibit a minor linear degradation (maximum 2 dBm) of the RSSI with the cadence. However, this has no significant impact on the packet loss, which remains relatively stable for each node throughout the experiments, as shown in Fig. 9c. The overall mean packet loss rates are 6.9, 8.9 and 7.9% for the thigh, shank and foot node, respectively.

Based on these results we can conclude that the pedaling cadence does not significantly impact on the packet lass rate and that the FastMAC protocol is robust enough to handle sudden drops in the RSSI values. The packet losses occur due to motion, as in the static situation we register loss rates of less than 0.1%. A more detailed analysis of the packet losses indicates that they occur in bursts, with 4 consecutive packets lost on average.

6 Discussion

There are several points of discussion related to the solution and results presented so far.

6.1 Advantages

The major progress beyond state-of-the-art is that such a miniaturized sensing system can assist cyclists outdoors, during training or racing. No wires, simple strap-on and instant feedback represent thus direct key benefits for the users. Additionally, the human movement and sports scientists are provided with extensive insight into the body kinematics in real-life conditions.

6.2 Limitations

Portable sensors are required to be as small as possible, which translates into a number of resource limitations related to: battery capacity, computational power, sensing accuracy, robustness of wireless communication. All these factors impact negatively on the system accuracy. In addition, compared to camera-based systems, inertial measurement solutions suffer from the inherent problem of error accumulation via integration and possibly from the approximations introduced in the reset step.

6.3 Assumptions in the reset step

In Sect. 3.2, we made the assumption that the pitch angle does not change at peaks. To backup this assumption, we compute the absolute difference between the minimum and the maximum pitch angles that the Optotrak system measures at peaks during all experiments. This absolute difference is 4° on average, which has negligible influence in the rotation matrix in Eq. 4.

6.4 Accuracy improvements

Different phases of our method can be improved:

- The calibration procedure of the inertial sensors can be extensively elaborated, for example as described in [12]. However, this requires dedicated laboratory equipment and much more time, thus cancelling the advantage of a simple-to-use portable system.
- The integration step (see Eq. 5) lacks the information related to the z axis of the gyroscope. Having a 3D gyroscope sensor on-board would solve this problem and enhance the overall accuracy.
- The reset method can be improved by fusing the information from the gyroscope sensors and the bike velocity (e.g. as input from the bike electronic equipment such as [5]). From the accelerometer signal, the rotational and translational accelerations can thus be removed. We can obtain therefore only the projection of the gravity force on the three axes, which can be used to compute the orientation.

6.5 Filtering

Filtering is the usual choice for improving the accuracy of inertial measurements. For example, Kalman filtering has been extensively used in related work for achieving a stable, drift-free performance [9, 10]. However, we are less considering filtering for improving our solution, due to:

- The high computational complexity and power consumption.
- The smoothening effect on the signal, which affects the angle peak values.
- The induced delay.

6.6 Energy consumption

The lifetime of the battery-powered sensor nodes is a constant concern. ProMove consumes approximately 40 mA in full-sampling (8 channels at 250 Hz) and communication mode. On a battery of 1,500 mAh, this translates to more than 36 h of uninterrupted functioning. If the system is used 8 h per day, batteries should be charged once in 4 days.

6.7 Lessons learned

Firstly, our experiments showed the net advantage in usability when using wireless sensor nodes compared to the

camera system. The complex set-up procedures, installation of wires and markers, as well as the confinement to a limited space in the lab, made the experiments with the camera system extremely laborious. In contrast, the sensor nodes required only a few minutes for calibration and mounting, after which the data could be immediately collected and processed. Secondly, the performance evaluation shows that lightweight algorithms, which are simple enough to run on low-power micro-controllers, can achieve a satisfactory degree of accuracy. Complex filtering might not always be needed, depending on the application specifics. Thirdly, it would be of much interest to determine the actual performance of our method in real-life, outdoors cycling. However, the main difficulty in achieving this is the impossibility of using camera systems in real-life conditions, in other words the lack of a reliable reference system. Finally, a point of attention in our solution remains the effect of magnetic disturbances. The lab in which the experiments were conducted exhibited such disturbances, which were partly compensated through calibration. We can expect accordingly a possible increase of accuracy in outdoors conditions.

6.8 Usability

We interviewed professional cyclists, cycling coaches and sport scientists from Australia and The Netherlands to find out if such a system would be of interest to professional riders and to get a view on the look-and-feel and the type of feedback the system should provide. They all agreed with the potential of the system for performance enhancement and overuse injuries prevention. The system offers an appealing solution to analyse the evolution of the lower limb kinematics over time, especially for an early detection of changes occurring at the onset of fatigue.

The system could be used to provide visual feedback allowing fatigue-induced alterations of the pedalling technique to be detected so that cyclists can continuously adjust their pedalling technique to maintain a high level of performance and limit the risk of injuries during training sessions and races. Future developments of the sensing system will be undertaken to reduce the size of the sensors and integrate them into the cyclists's clothing and/or bikes. Simple and instantaneous visual feedback about pedalling technique could be displayed through the miniaturized bike computers fixed to the handlebars of the bikes used by cyclists. An important suggestion recurring in most interviews was to integrate the information related to kinematic parameters with power measurements from existing commercial systems (e.g. SRM). The ideal system would be composed of several dedicated wireless sensors, such as the ProMove nodes, but smaller and integrated into clothing and bike, and one bike computer or mobile device that can fuse kinematic information with power measurements in order to provide feedback to the cyclist.

7 Conclusions and future work

We presented the design of a portable wireless sensor network that can be used for real-time monitoring of lower-limb kinematics during cycling. Due to the importance of the joint kinematics to assess the cycling technique, we focus on measuring the knee and ankle joint angles. We performed a series of experiments with nine subjects to assess the accuracy of our system compared to the gold-standard camera-based systems. Results show an accuracy between 2.2° and 6.4°, with a correlation coefficient above 0.9, which demonstrate a good performance of our system. Furthermore, we show that the wireless communication is robust enough to handle sudden drops in the RSSI values and that the energy consumption gives the sensor network a life-span of a couple of days, thus being suitable for a wearable system.

The solution proposed is not constrained to cycling only. The algorithm for orientation computation can be applied, with minor optimizations, for any generic cyclic or repetitive motion. This opens perspectives for use in a number of sports, such as rowing, swimming, skating, running, skiing.

This work represented the starting point of an on-going international collaboration, substantiated so far in two research projects: one investigating the generic use of wireless motion sensor networks in sports (The Netherlands) and one focusing on the development of an extended system for measuring pedalling technique in real-life conditions (Australia). This collaboration will allow us to further evaluate the performance, reliability and usability of our solution in real-life conditions.

References

1. Martin JC, Brown NAT (2009) Joint-specific power production and fatigue during maximal cycling. J Biomech 42(4):474–479
2. Silberman MR, Webner D, Collina S, Shiple BJ (2005) Road bicycle fit. Clin J Sport Med 15(4):271–276
3. Sauer JL, Potter JJ, Weisshaar CL, Ploeg H, Thelen DG (2007) Influence of gender, power and hand position on pelvic motion during seated cycling. Med Sci Sports Exer 39(12):2204–2211
4. Dingwell JB, Joubert JE, Diefenthaeler F, Trinity JD (2008) Changes in muscle activity and kinematics of highly trained cyclists during fatigue. IEEE Trans Biomed Eng 55(11):2666–2674

5. Polar equipment. http://www.polar.fi
6. Bouhafs F, Merabti M, Mokhtar H (2007) The BikeNet mobile sensing system for cyclist experience mapping. In: SenSys. ACM, New york, pp 87–101
7. Optotrak Certus Motion Capture System. http://www.ndigital.com
8. Dejnabadi H, Jolles BM, Aminian K (2005) A new approach to accurate measurement of uniaxial joint angles based on a combination of accelerometers and gyroscopes. IEEE Trans Biomed Eng 52(8):1478–1484
9. Luinge HJ, Veltink PH (2005) Measuring orientation of human body segments using miniature gyroscopes and accelerometers. Med Biol Eng Comput 43(2):273–282
10. Zhu R, Zhou Z (2004) A real-time articulated human motion tracking using tri-axis inertial/magnetic sensors package. IEEE Trans Neural Syst Rehabil Eng 12(2):295–302
11. Roetenberg D, Slycke PJ, Veltink PH (2007) Ambulatory position and orientation tracking fusing magnetic and inertial sensing. IEEE Trans Biomed Eng 54(5):883–890
12. Morris SJ (2004) A shoe-integrated sensor system for wireless gait analysis and real-time therapeutic feedback. PhD thesis, Massachusetts Institute of Technology
13. Findlow A, Goulermas JY, Nester C, Howard D, Kenney LPJ (Nov. 2007) Predicting lower limb joint kinematics using wearable motion sensors. Gait and Posture, pp 120–126
14. Takeda R, Tadano S, Natorigawa A, Todoh M, Yoshinari S (July 2009) Gait posture estimation using wearable acceleration and gyro sensors. J Biomech
15. ProMove wireless inertial sensing platform. http://www.inertia-technology.com
16. Tuck K (2007) Tilt sensing using linear accelerometers. Freescale Semiconductor Application Note AN3107
17. Caruso MJ (1997) Applications of magnetoresistive sensors in navigation systems. SAE Trans 106(6):1092–1098
18. Farrell JA, Barth M (1998) The global positioning system and inertial navigation. McGraw-Hill Professional, New York
19. Bosch S, Marin-Perianu M, Marin-Perianu RS, Scholten J, Havinga PJM (2009) Followme! Mobile team coordination in wireless sensor and actuator networks. In: PerCom, pp 151–161
20. Cappozzo A, Croce U Della, Leardini A, Chiari L (2005) Human movement analysis using stereophotogrammetry. Part 1: theoretical background. Gait Posture 21(2):186–196
21. Visual3D Advanced Biomechanics Research Software for 3D Motion Analysis. http://www.c-motion.com
22. Marin-Perianu M, Chatterjea S, Marin-Perianu RS, Bosch S, Dulman SO, Kininmonth S, Havinga PJM (2008) Wave monitoring with wireless sensor networks. In: ISSNIP, pp 611–616
23. Caruso MJ (2000) Applications of magnetic sensors for low cost compass systems. IEEE position location and navigation symposium, pp 177–184
24. Cycling with wireless motion sensors. Demonstration video. http://www.youtube.com/watch?v=NVJXRPt6SvY